Impacts of parameterized orographic drag on the Northern Hemisphere winter circulation

AGU PUBLICATIONS

Journal of Advances in Modeling Earth Systems

RESEARCH ARTICLE
10.1002/2015MS000564

Impacts of parameterized orographic drag on the Northern Hemisphere winter circulation

Irina Sandu[1], Peter Bechtold[1], Anton Beljaars[1], Alessio Bozzo[1], Felix Pithan[2], Theodore G. Shepherd[2], and Ayrton Zadra[3]

[1]European Centre for Medium-Range Weather Forecasts, Reading, UK, [2]University of Reading, Reading, UK, [3]Environment Canada, Dorval, Quebec, Canada

Key Points:
- Parameterized orographic drag affects the Northern Hemisphere winter circulation at all time scales
- The partition of the surface stress between various parameterizations affects circulation aspects

Correspondence to:
I. Sandu,
irina.sandu@ecmwf.int

Citation:
Sandu, I., P. Bechtold, A. Beljaars, A. Bozzo, F. Pithan, T. G. Shepherd, and A. Zadra (2016), Impacts of parameterized orographic drag on the Northern Hemisphere winter circulation, *J. Adv. Model. Earth Syst.*, *7*, doi:10.1002/2015MS000564.

Received 15 OCT 2015
Accepted 21 DEC 2015
Accepted article online 26 DEC 2015

Abstract A recent intercomparison exercise proposed by the Working Group for Numerical Experimentation (WGNE) revealed that the parameterized, or unresolved, surface stress in weather forecast models is highly model-dependent, especially over orography. Models of comparable resolution differ over land by as much as 20% in zonal mean total subgrid surface stress (τ_{tot}). The way τ_{tot} is partitioned between the different parameterizations is also model-dependent. In this study, we simulated in a particular model an increase in τ_{tot} comparable with the spread found in the WGNE intercomparison. This increase was simulated in two ways, namely by increasing independently the contributions to τ_{tot} of the turbulent orographic form drag scheme (TOFD) and of the orographic low-level blocking scheme (BLOCK). Increasing the parameterized orographic drag leads to significant changes in surface pressure, zonal wind and temperature in the Northern Hemisphere during winter both in 10 day weather forecasts and in seasonal integrations. However, the magnitude of these changes in circulation strongly depends on which scheme is modified. In 10 day forecasts, stronger changes are found when the TOFD stress is increased, while on seasonal time scales the effects are of comparable magnitude, although different in detail. At these time scales, the BLOCK scheme affects the lower stratosphere winds through changes in the resolved planetary waves which are associated with surface impacts, while the TOFD effects are mostly limited to the lower troposphere. The partitioning of τ_{tot} between the two schemes appears to play an important role at all time scales.

1. Introduction

The drag exerted by the Earth surface on the atmospheric flow has long been recognized to play an important role in the general circulation of the atmosphere [*Holton*, 2004]. This follows from considerations related to the angular momentum budget, which leads to a picture of angular momentum fluxes in the free troposphere balancing surface drag and explains the presence of surface easterlies in the tropics and surface westerlies in the midlatitudes. Although it is clear that the magnitude of the surface stress controls the strength of the surface easterlies and westerlies, it has also, more surprisingly, been shown to affect the location of the surface westerly jet in the midlatitudes [*Robinson*, 1997; *Chen et al.*, 2007].

Moreover, the drag exerted by topography is particularly important for the Northern Hemisphere (NH) winter extratropical circulation. The stationary Rossby (or planetary) waves forced by the flow over the Himalayas and Rockies were shown to explain the winter mean longitudinal distribution of 500 hPa heights in the NH midlatitudes [*Charney and Eliassen*, 1949; *Held et al.*, 2002]. The drag exerted by orographically generated gravity waves has also been shown to affect the NH winter zonal mean flow both in the troposphere and the lower stratosphere since the early days of weather and climate prediction [*Wallace et al.*, 1983; *Palmer et al.*, 1986; *McFarlane*, 1987]. These early studies emphasized the importance of parameterizing orographic gravity wave effects in General Circulation Models (GCMs) in order to reproduce the observed mean patterns of the NH winter circulation. Later studies demonstrated that the orographic gravity wave drag affects the zonal mean flow by changing the resolved planetary waves [*McLandress and McFarlane*, 1993; *Shaw et al.*, 2009; *Sigmond and Scinocca*, 2010]. Orography also exerts drag on the atmosphere by blocking the flow at low levels. The parameterization of such orographic low-level blocking effects influences the representation of the NH winter circulation in both weather forecast and climate simulations [*Lott and Miller*, 1997; *Zadra et al.*, 2003; *Sandu et al.*, 2013a, 2013b; *Pithan et al.*, 2015].

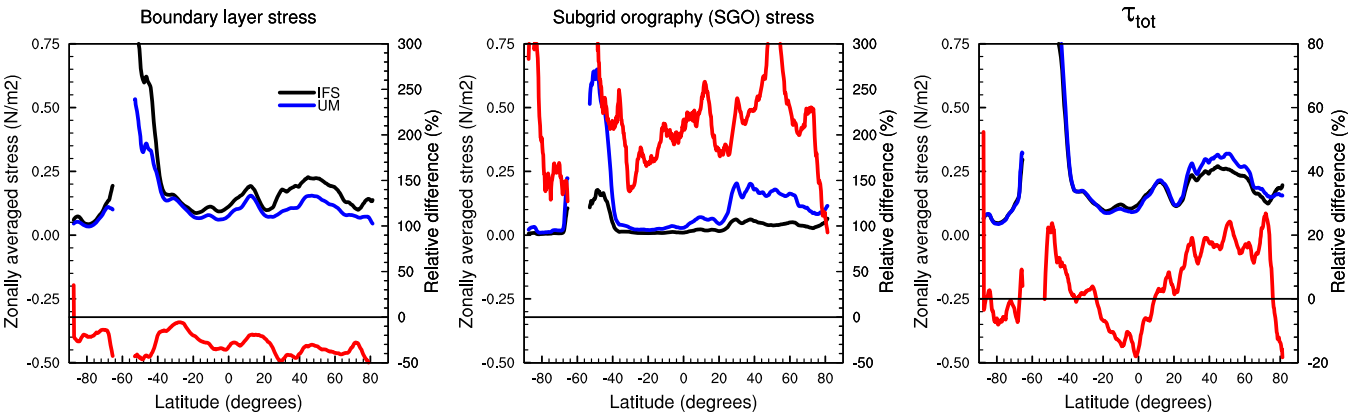

Figure 1. Zonal averages of the magnitude of the total subgrid surface stress τ_{tot} (N/m^2) and of its components for IFS (black, scale on left) and UM (blue, scale on left), from the results submitted for the WGNE Drag project for January 2012, and relative difference between UM and IFS (red, scale on right). For IFS, the boundary layer stress (left) represents the sum of the stresses from the turbulence and turbulent orographic form drag schemes; for UM it represents the stress from the turbulence scheme which represents the orographic form drag implicitly through an orographic enhancement of the roughness (see section 2 for details). For comparison with the results from the WGNE Drag project, the magnitude of the stress used to construct the zonal averages is computed in this plot only from monthly mean diurnal averages of the u and v components of the surface stress (derived from the first 24 h of the daily 00UTC forecasts). The zonal averages include only land grid cells and were smoothed using a 5° running mean. The lines present gaps at ocean only latitudes.

Albeit recognized as being important for both weather forecasts and climate simulations, the representation of drag processes associated with surface stress is a major source of uncertainty in GCMs. Parameters controlling their strength are poorly constrained and often tuned to obtain the desired model behavior, i.e., forecast skill [*Sandu et al*., 2013a, 2013b] or mean climate [*Pithan et al*., 2015]. The uncertainty not only stems from the lack of observational constraints, but also from the fact that surface stress has received relatively little attention compared to other processes such as clouds, convection, or radiation.

In the last couple of years, the interest in the surface momentum budget has increased, particularly in the framework of the World Meteorological Organization's Working Group for Numerical Experimentation (WGNE) and of a workshop on the "Momentum Budget and its Role in Weather and Climate" organized in March 2015 at Eynsham Hall, United Kingdom. In 2014, WGNE set up a model intercomparison exercise of subgrid (or unresolved) surface stress, the WGNE Drag project. This exercise aims to compare the total subgrid surface stress (τ_{tot}) and its partitioning among the parameterizations that most models use to represent it: the boundary layer scheme and the subgrid orography scheme (section 2 will provide more details on the representation of subgrid surface stress in models). Monthly mean zonal and meridional subgrid surface stresses from the first 24 h of short-range forecasts performed for January and July 2012 were gathered from 12 modeling groups [*Zadra*, 2015]. Since the models forecasts were starting from similar initial states, the angular momentum fluxes in the free atmosphere can be presumed to be similar and one would then expect similar total surface stresses.

First results of this exercise suggest that while the intermodel spread is relatively small over the oceans, τ_{tot} is highly model-dependent over land [*Zadra*, 2015]. As the subgrid, or parameterized stress characterizes the unresolved part of the flow, the intermodel spread found over land is due in part to differences in horizontal resolution. Nevertheless, the zonally averaged magnitude of τ_{tot} can still differ by as much as 20% over land even for models of comparable resolution, such as the Integrated Forecast System (IFS) of the European Centre for Medium-Range Weather Forecasts (ECMWF) and the Unified Model (UM) of the MetOffice (Figure 1). These differences in the zonal average stress are mostly related to differences in stress over orography (not shown). Moreover, the partition of τ_{tot} between the boundary layer and subgrid orography schemes is also model-dependent. The UM for example has almost twice as much subgrid orography stress and up to 50% less boundary layer stress than IFS in the NH (Figure 1). Finally, the WGNE Drag project also revealed that the diurnal cycle of τ_{tot} is quite different among the models (not shown).

The ongoing WGNE Drag project emphasizes the importance of better constraining the representation of subgrid surface stress in models, especially in regions with orography. It also highlights the need to better understand how the schemes contributing to surface stress, and their uncertainties, affect weather and

climate predictions. The present study looks into a particular aspect of this broader question, namely how some of these schemes impact the representation of the NH winter circulation on different time scales. More precisely, our study aims to address two of the questions raised by the WGNE Drag project, namely (i) whether differences in τ_{tot} of the order of those revealed by the WGNE Drag project matter for the representation of the NH winter circulation, and (ii) whether the partitioning of τ_{tot} between the different schemes in a particular model is also important for predicting certain circulation aspects. As most of the uncertainty in surface stress comes from regions with orography, we focus on the impacts of two of the schemes which represent orographic drag processes.

To answer these questions, we use the IFS to perform both 10 day weather forecasts and seasonal integrations, in which we mimic an increase in τ_{tot} that is comparable to the difference between the IFS and the UM shown in the WGNE Drag project. This increase is simulated in two ways, namely by changing a poorly constrained parameter either in the boundary layer or in the subgrid orography scheme. Both changes concern the representation of subgrid orographic drag exerted on the flow at low levels. The representation of the subgrid surface stress in the IFS is described in section 2. The setup of the experiments is presented in section 3. Section 4 discusses the impacts of the changes to subgrid orographic drag on the representation of the NH winter circulation in short and medium-range forecasts. Particular emphasis is put on whether these impacts are different depending on which of the parameterizations is modified. Section 5 includes a similar discussion for the seasonal integrations.

2. Representation of Subgrid Surface Stress in the IFS

Models often use more than one scheme to represent subgrid stress. The reason is that different schemes parameterize different drag-related processes. In the IFS the boundary layer scheme represents stress associated with unresolved elements of the Earth surface from horizontal scales less than 5 km, while the subgrid orography scheme (SGO) represents stress associated with horizontal scales between 5 km and the model resolution. The 10 day weather forecasts and the seasonal integrations discussed in this study are performed at horizontal resolutions of approximately 32, respectively, 75 km at the Equator (section 3).

At their turn, each of these two schemes represents several processes. Thus, the boundary layer scheme uses a turbulence parameterization (TURB hereafter) to represent turbulent drag associated with surface elements such as land use or vegetation. The TURB scheme is based on Monin Obukhov similarity and uses prescribed roughness length tables to describe the characteristic height of these surface elements [*IFS documentation*, 2015, part IV]. The boundary layer scheme also includes a turbulent orographic form drag parameterization (TOFD hereafter) to represent drag associated with subgrid orography elements with horizontal scales less than 5 km such as hills or individual mountains [*Beljaars et al*., 2004]. The TOFD stress is formulated in terms of the variance of the terrain slope, which is derived from an empirical representation of the height spectrum in the scale range of 5 km to a few meters (this spectrum is derived from a 1 km resolution elevation data set). The vertical distribution of the stress is prescribed on model levels according to the formulation proposed by *Wood et al*. [2001]. It is worth noting that this scheme does not consider stability effects. Other models (e.g., the UM of the Metoffice) do not have a special parameterization for turbulent orographic form drag, but represent it by artificially enhancing the surface roughness length over orography, so that the orographic form drag is implicitly represented by the turbulence parameterization. The impact of either the TOFD parameterization or the orographic enhancement of roughness is poorly documented in the literature [*Wallace et al*., 1983], although it has been shown to affect the NH wintertime circulation to some extent [*Sandu et al*., 2013a, 2013b].

The SGO scheme [*Lott and Miller*, 1997] also represents different types of drag. If the airflow has enough energy to pass over the so-called effective subgrid mountain height, orographic gravity waves are generated. The subgrid stress associated with the propagation and breaking of these waves is represented by the gravity wave drag component of the SGO scheme (GWD hereafter). At low levels, where the flow does not have enough energy, the air goes around the mountain. The stress induced by this process is described by the low-level blocking component of the SGO scheme (BLOCK hereafter). The depth over which the flow is blocked, and goes around the mountain, controls to a large extent the effect of the BLOCK scheme. This blocking depth is equal to the subgrid mountain height minus the depth of the layer where the flow goes over the mountain (and generates gravity waves). The depth of this latter layer is defined by a critical

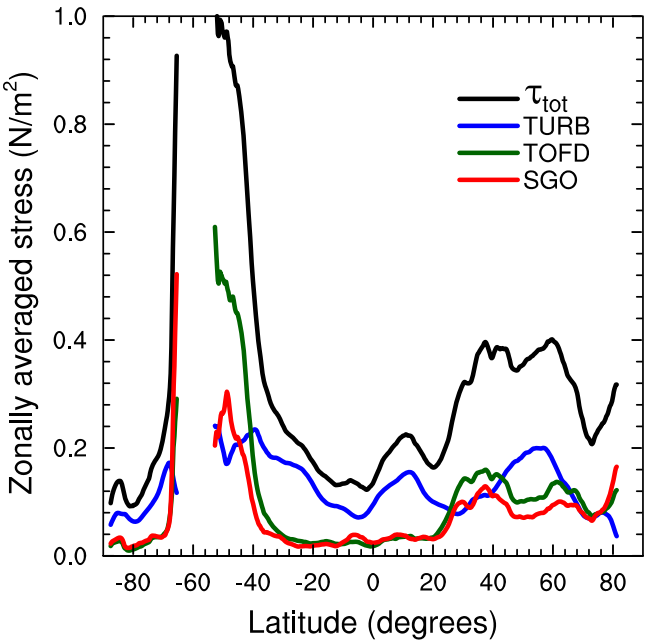

Figure 2. Zonal averages of the magnitude of τ_{tot} and of the contributions of the TURB, TOFD, and SGO schemes to τ_{tot} (N/m^2) for the CTL experiment. These zonal averages are computed from monthly means of daily surface stress magnitude (derived from the first 24 h of the daily 00UTC forecasts performed for February 2014), include only land grid cells and were smoothed using a 5° running mean. The lines present gaps at ocean only latitudes.

Froude number which makes both the gravity wave amplitude and the blocking depth stability dependent. For strong flow and/or weak stability, the gravity wave amplitude is large and the blocking depth is small, whereas for weak flow and very stable stratification the gravity wave amplitude is small and the blocking height large. Other models use similar schemes to represent gravity wave drag and low-level blocking effects [e.g., *McFarlane*, 1987; *Webster et al*., 2003; *Brown and Webster*, 2004], and some include an "orographic lift" component, which describes a force perpendicular to the flow that depends on the wind direction relative to the orientation of the subgrid orography [*Lott*, 1999].

The contributions of the GWD and BLOCK schemes to the subgrid surface stress cannot be disentangled in IFS, so they are presented combined hereafter as the SGO contribution to τ_{tot}. Special diagnostics were added for the purpose of this study within the boundary layer scheme in order to separate the contributions of the TURB and TOFD schemes to τ_{tot}.

Figures 2 and 3 show how much each of these schemes contributes to τ_{tot} in short-range forecasts performed with the IFS for February 2014 (the experimental setup is described in more detail in section 3). In zonal average, the TOFD and SGO schemes contribute fairly equally over land to the magnitude of τ_{tot} (Figure 2). Their contribution is comparable to that of the TURB scheme at latitudes with a fair amount of orography (e.g., mid to high latitudes in the NH). However, the maps shown in Figure 3 indicate that the schemes act in different regions. The TOFD and SGO act as expected in regions with orography, while the TURB scheme acts predominantly in regions with increased synoptic activity (i.e., storm tracks) and its contribution to τ_{tot} over orography is small. These figures only illustrate 24 h averages of the monthly mean magnitude of the surface stress, ignoring thus differences in the diurnal cycle. However, as it will be shown in the next section, the stress produced by the various schemes has also different diurnal cycles.

The results illustrated here for the IFS cannot be generalized. The WGNE Drag project demonstrated that τ_{tot} and its partition among the different schemes is largely model-dependent, particularly in regions with orography [*Zadra*, 2015]. Moreover, individual model results heavily depend on the assumptions and choices of parameter values made within the schemes contributing to τ_{tot}. Given that it is currently not possible to constrain either τ_{tot} or its orographic component with observations on global, and even on regional scale, the assumptions and parameter choices often rely on a rather pragmatic optimization approach. In previous work [*Sandu et al*., 2013a, 2013b], we showed that the medium-range forecast skill for the geopotential height during the NH winter can be improved by combining changes to the TURB scheme concerning the degree of turbulent diffusion in stable layers with changes to certain parameters of the TOFD and BLOCK schemes.

3. Experimentation

In the present study, we look in more detail at the individual impacts of the TOFD and BLOCK schemes on the NH winter circulation. These two schemes are likely the most poorly constrained and less documented in terms of impacts on the large-scale circulation. Given that they represent similar processes contributing

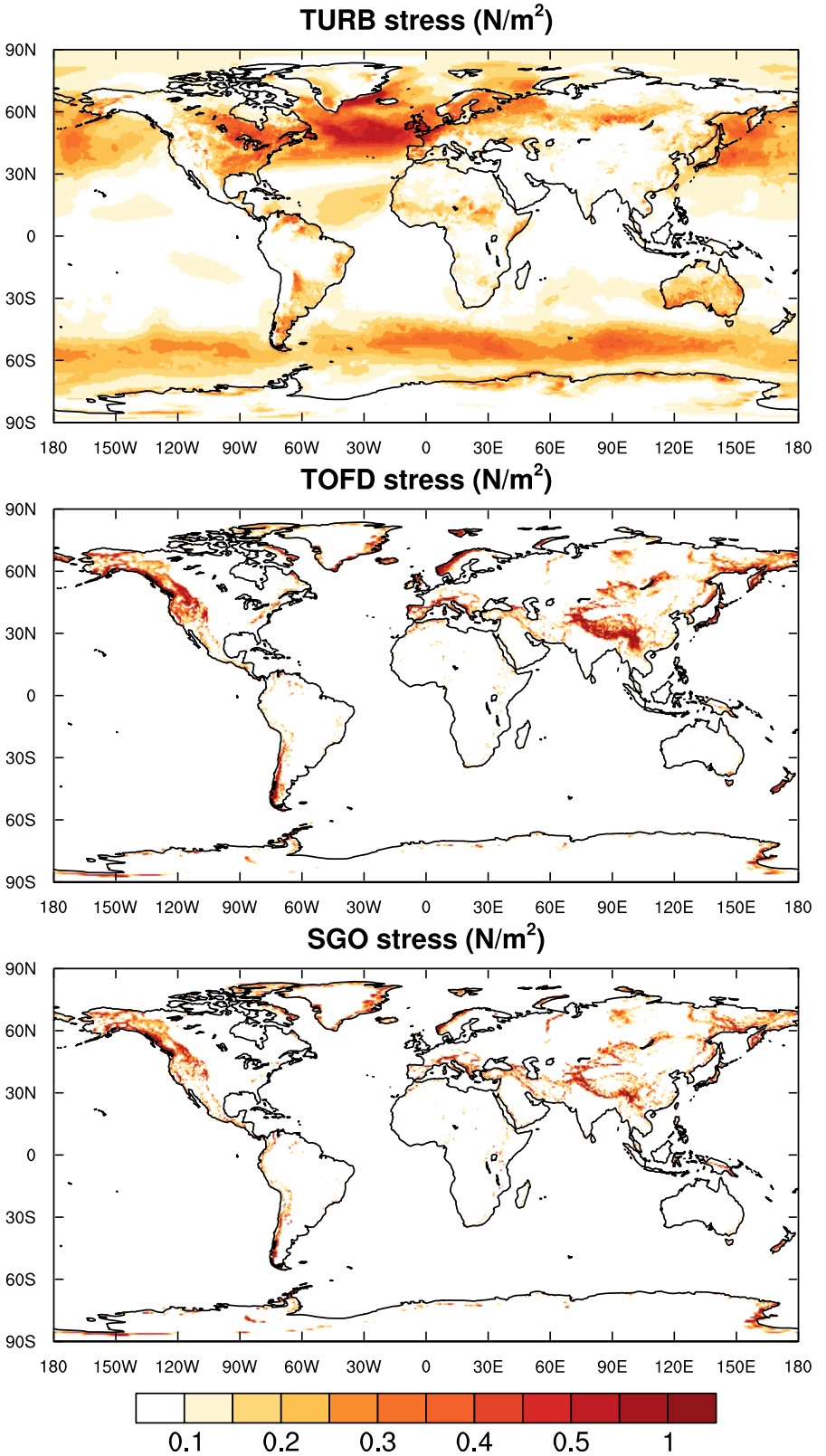

Figure 3. Magnitude of the surface stress due to the TURB, TOFD, and SGO schemes (N/m^2) for the CTL experiment. These fields represent monthly means of the daily surface stress magnitude, derived from the first 24 h of the daily 00UTC forecasts performed for February 2014.

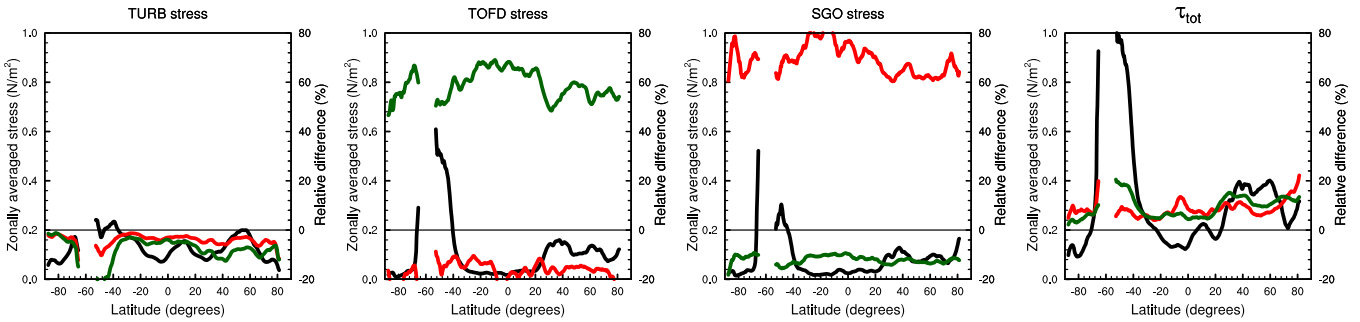

Figure 4. Zonal averages of the magnitude of τ_{tot} (right) and of the contributions of the TURB, TOFD, and SGO schemes to τ_{tot} (from left to right) (N/m^2) for the CTL experiment (black, scale on left). The green and red curves, scale on right, show the relative change of τ_{tot} and of its components in the experiments H-TOFD and H-BLOCK with respect to the CTL. The zonal averages are computed as in Figure 2.

to the surface stress (orographic drag at low levels), these schemes also constitute good candidates for exploring the role of the partitioning of τ_{tot} between different schemes.

Two types of experiments are performed to answer the questions we focus on. First, daily 10 day forecasts starting at 00UTC are performed for February 2014. The forecasts start from the ECMWF operational analysis and are performed with a vertical resolution of 137 levels at a linear spectral truncation of T639 corresponding to approximately 32 km at the Equator. Second, seasonal integrations are performed with the same number of vertical levels, but at a lower spectral resolution, i.e., T255 corresponding to approximately 75 km at the Equator. These runs are initialized with the ECMWF Interim reanalysis ERAI [*Dee et al*., 2011]. They start on 1 August for every year between 1984 and 2014 and are integrated over a period of 7 months. This setup allows to examine the climate of the model during the winter season, December-January-February (DJF), and its response to changes in subgrid orographic drag. The most recent operational IFS cycle (CY41R1 operational since May 2015) is used for all experiments.

For each of these two types of runs, we perform a control experiment with the reference model, an experiment with a larger magnitude of the stress resulting from the TOFD scheme and an experiment with a larger magnitude of the stress resulting from the BLOCK scheme. The 10 day forecast experiments will be denoted as CTL, High TOFD (H-TOFD), and High BLOCK (H-BLOCK) hereafter, while the seasonal integrations will be denoted as CTL-CL, H-TOFD-CL, and H-BLOCK-CL.

The magnitude of the stress resulting from each scheme is enhanced by increasing the value of one of its poorly constrained constant factors, α_{tofd} for the TOFD scheme and C_d in the BLOCK scheme. These factors scale the stress (τ) in the two schemes as follows:

$$\tau_{TOFD} \sim \alpha_{TOFD}\rho\vec{U}|\vec{U}|f_{TOFD} \qquad \tau_{BLOCK} \sim C_D\rho\vec{U}|\vec{U}|f_{BLOCK}, \tag{1}$$

where ρ is the air density, $\vec{U}$ the horizontal wind vector, f_{TOFD} is a function of the standard deviation of the filtered subgrid orography, and f_{BLOCK} is function of stability, the characteristics of the subgrid orography (i.e., standard deviation, slope, and anisotropy) and the direction of the flow with respect to the mountain ridges (a detailed description of the two schemes is included in *IFS documentation* [2015, chap. 3.4 and 4, Part IV]).

The changes are such that they lead to a similar increase in the zonally averaged magnitude of τ_{tot} (defined as in the caption of Figure 2) in the short range of the H-TOFD and H-BLOCK forecasts. Furthermore, this increase is similar to the difference between the IFS and the UM (Figure 1). Thus, the increase in zonal mean τ_{tot} in the H-TOFD and H-BLOCK experiments is of approximately 10–15% in the NH midlatitudes (Figure 4), while the difference between the IFS and UM in the WGNE Drag project was of about 15–20% (Figure 1). Also note that an increase in the stress from any of the schemes leads to a reduction in near surface wind, which further results in a small reduction of the stress produced by the other schemes (Figure 4). In the H-TOFD experiment for example, the TOFD stress increases by approximately 60%, while the TURB and SGO stress each decrease by 10%.

By design the zonally averaged magnitude of τ_{tot} increases by a similar amount in the NH midlatitudes in the H-TOFD and H-BLOCK experiments. However, a zoom on the τ_{tot} increase in the Himalaya region reveals that the TOFD scheme enhances the stress over a larger area than the BLOCK scheme, which seems to act

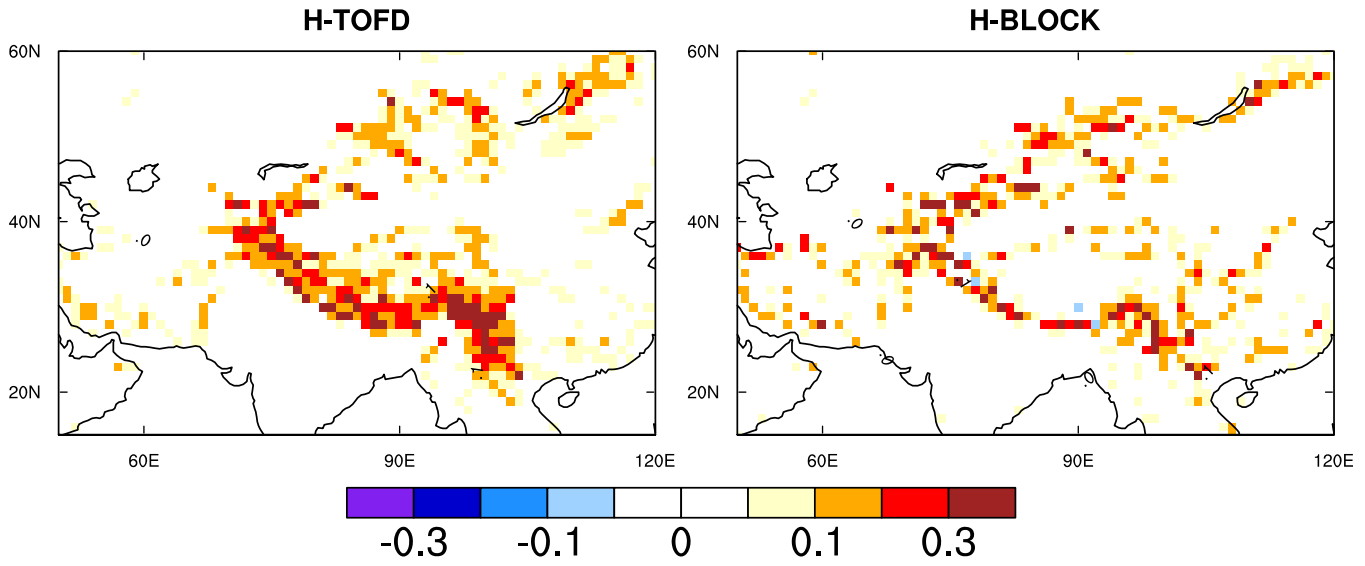

Figure 5. Monthly mean difference in the daily magnitude of τ_{tot} (N/m^2) between the H-TOFD (left), respectively, H-BLOCK (right) and the CTL experiment.

more near the edges of the mountain chain (Figure 5). Furthermore, Figure 6 reveals that the diurnal cycle of the increase in τ_{tot} is of opposite phase in the H-TOFD and H-BLOCK experiments. Thus, the increase in τ_{tot} is maximum for H-TOFD and minimum for H-BLOCK between 6 and 12 UTC (about 12–18 local time). This afternoon extreme can be explained as follows. In the afternoon the boundary layer is mostly unstable (or less stable) and the near-surface wind has a daily maximum due to strong turbulent mixing (not shown). Since the TOFD scheme responds to wind speed only, it will reflect the diurnal cycle of the surface wind. However, the BLOCK scheme responds not only to wind speed, but is also strongly modulated by stability mainly through the depth of the blocked layer. When the wind speed is high and stability is weak, the flow the layer where the flow goes over the mountain is deep and the remaining layer where the flow is blocked is shallow. Therefore, the H-BLOCK experiment shows a minimum increase in τ_{tot} during daytime.

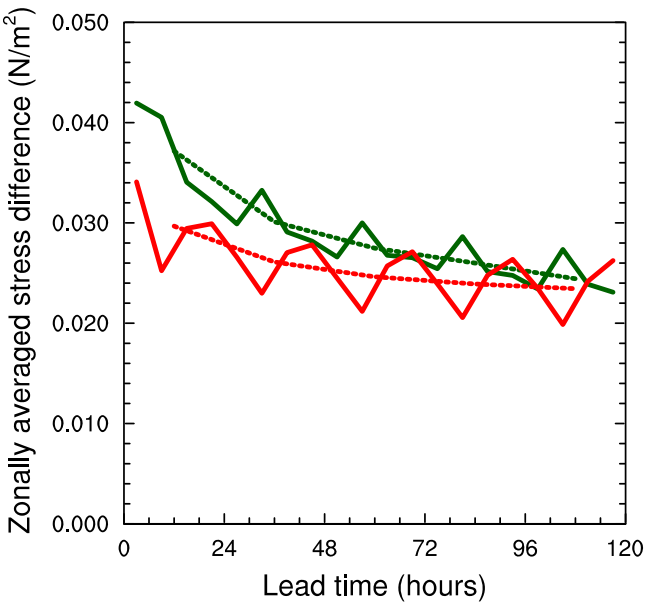

Figure 6. Time evolution of the monthly mean differences in the magnitude of τ_{tot} (N/m^2) between the H-TOFD (green), respectively, H-BLOCK (red) and the CTL experiment during the first 5 days of the forecasts performed for February 2014, integrated over the Himalaya area showed in Figure 5. Full lines indicated 6 h averages, and dashed lines indicate diurnal averages of the difference in the magnitude of τ_{tot}. The forecasts start at 00UTC.

In the next two sections, we examine the impacts of these two seemingly similar, yet different, ways of increasing τ_{tot} in a particular model. We seek to understand the consequences of these changes on the NH winter circulation, first on daily time scales and then at longer time ranges.

4. Impacts in Short and Medium-Range Weather Forecasts

Changes in surface pressure have traditionally been used to illustrate orography-related effects on the NH winter circulation since the first studies describing the parameterization of orographic gravity wave drag in GCMs [*Wallace et al.*, 1983; *Palmer et al.*, 1986; *McFarlane*, 1987]. The impact of enhancing the orographic drag at low levels in the H-TOFD and H-BLOCK 10 day forecast experiments is therefore

first assessed in terms of surface pressure changes at short and medium ranges (1–5 days). The impacts on the representation of the NH circulation are then discussed in terms of zonal wind, temperature, and geopotential height.

4.1. Short-Range Response in Surface Pressure

The enhancement of τ_{tot}, simulated by increasing either the TOFD or the BLOCK stress, leads to changes in the mean surface pressure in a matter of hours (Figure 7). Thus, pressure gradient changes across the regions with the largest mountain chains (Himalayas and the Rocky Mountains), as well as an increase in surface pressure over Europe, can already be observed within the first 6 h of the forecasts. During the first 24 h these changes amplify and extend to larger spatial scales in both experiments, although they are always stronger for the H-TOFD forecasts.

The short-range response in surface pressure over Europe is particularly intriguing because it does not clearly resemble the pattern of the pressure changes over North America and East Asia. This raises the question whether this is a local effect due to the Alps or Greenland or it is due to nonlocal effects caused by the changes in orographic drag over the Rockies or the Himalayas. More generally, the question is whether these changes in surface pressure in the short range are purely local orographic effects or are nonlocal effects due to impacts of the orographic drag on the zonal flow.

To answer this question we performed additional daily 10 day forecasts for February 2014. The changes made in the original H-TOFD and H-BLOCK experiments were this time applied only in selected regions of the globe. For each of the two schemes, three new experiments were thus run in which the stress was enhanced over regions covering North America, Greenland and Europe, and East Asia, illustrated by the green boxes in Figure 8.

The changes in surface pressure observed after 24 h over North America and East Asia in the new experiments (Figure 8, top, bottom) are virtually identical with those obtained in the original H-TOFD and H-BLOCK experiments (Figure 7). This suggests that the short-range effects in those regions are local. Over Europe the changes observed in the new experiments are also mainly due to a locally induced meridional pressure gradient (Figure 8, middle). The decrease in surface pressure seen East/South of the Alps in the experiment where the TOFD stress is enhanced over Greenland and Europe only (Figure 8, middle) is outweighed however in the original H-TOFD experiment (Figure 7) by the increase in pressure induced by the changes in stress over East Asia (Figure 8, bottom).

As suggested by *Zadra et al*. [2003], the local response in surface pressure over the largest mountain chains can be understood in terms of geostrophic balance. The induced meridional pressure gradient across the Rockies, Alps, and, respectively, Himalayas, corresponds to a westward geostrophic zonal wind anomaly, that is a deceleration of the midlatitude surface westerlies caused by the enhancement of the stress over orography. A decrease in the zonal surface wind of -1 to -0.2 m s^{-1} can be indeed seen on the west side of the mountain chains for all experiments (green hatches in Figure 8).

That changing the drag exerted by orography on the flow at low levels leads to a rapid response in surface pressure is hardly a surprise, given our current understanding (*Zadra et al*., 2003). What is interesting instead is that although the changes made to the two schemes lead to a similar zonally averaged change in τ_{tot}, the magnitude of the response in surface pressure is rather different (Figure 7). One possibility is that differences in the spatial distribution and the diurnal cycle of τ_{tot} (Figures 5 and 6) lead to a different response in surface pressure. The other possibility is that this response is damped to some extent in the H-BLOCK experiment due to the interactions between the GWD and BLOCK parameterizations. Indeed, the low-level blocking and gravity wave drag are both represented in the SGO scheme. Therefore, it is impossible to tell a priori whether a change of the stress at low levels, such as that simulated in the H-BLOCK experiment, does not also affect the orographic gravity waves. If this was the case, the changes in surface pressure obtained in the H-BLOCK experiment could be due at least in part to changes in the propagation and breaking of the gravity waves. To investigate this possibility, we repeated the CTL and H-BLOCK experiments while turning off the GWD part of the SGO scheme. The difference in mean surface pressure between these two new experiments matches closely that between the original H-BLOCK and CTL experiments shown in Figure 7. This suggests that the response obtained in the short range of the H-BLOCK forecasts is actually due to low-level blocking effects.

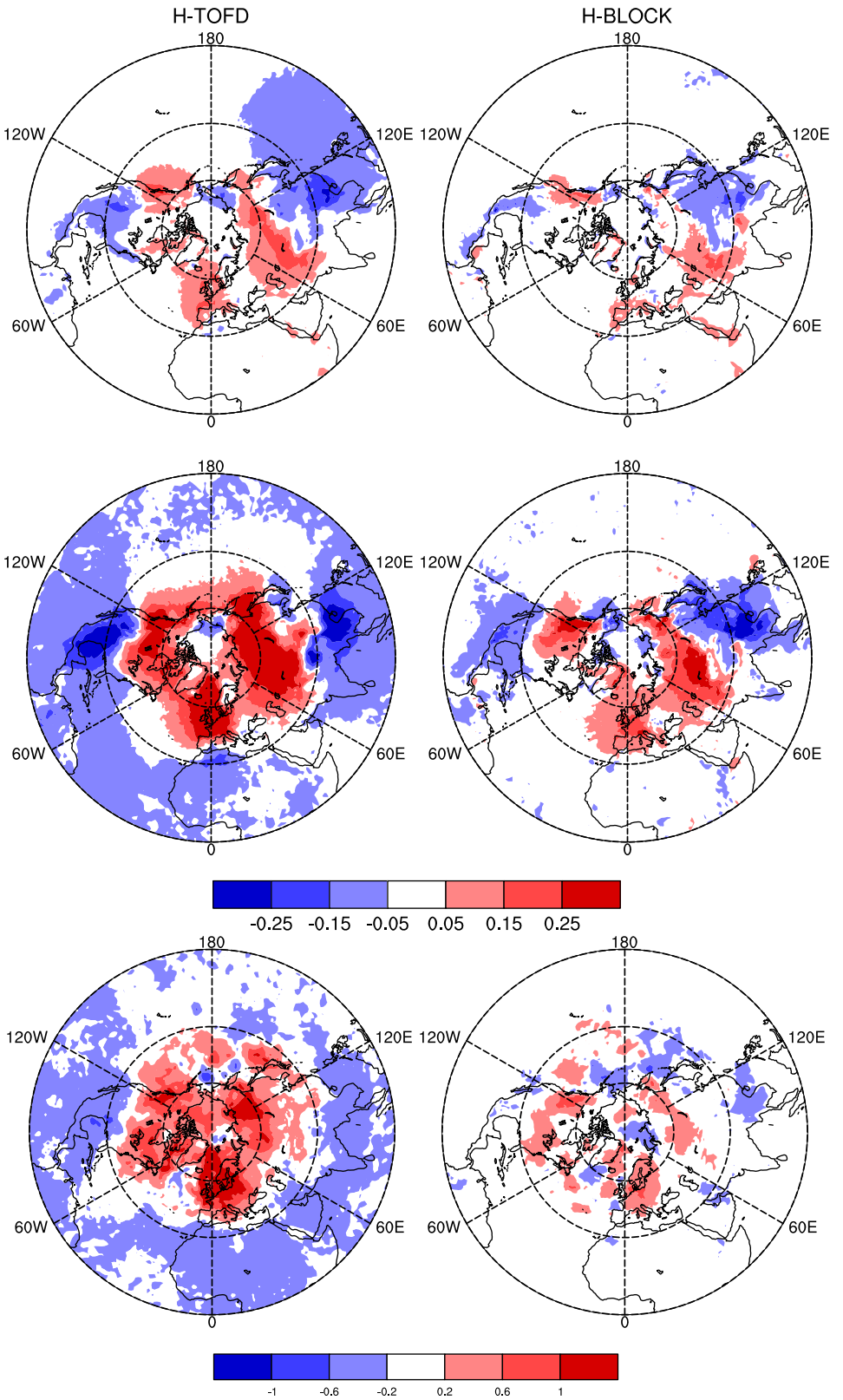

Figure 7. Mean change in surface pressure (hPa) in the experiments H-TOFD (left) and H-BLOCK (right) with respect to the CTL, at lead time 6 (top), 24 (middle), and 120 (bottom) hours of the daily 00UTC forecasts performed for February 2014.

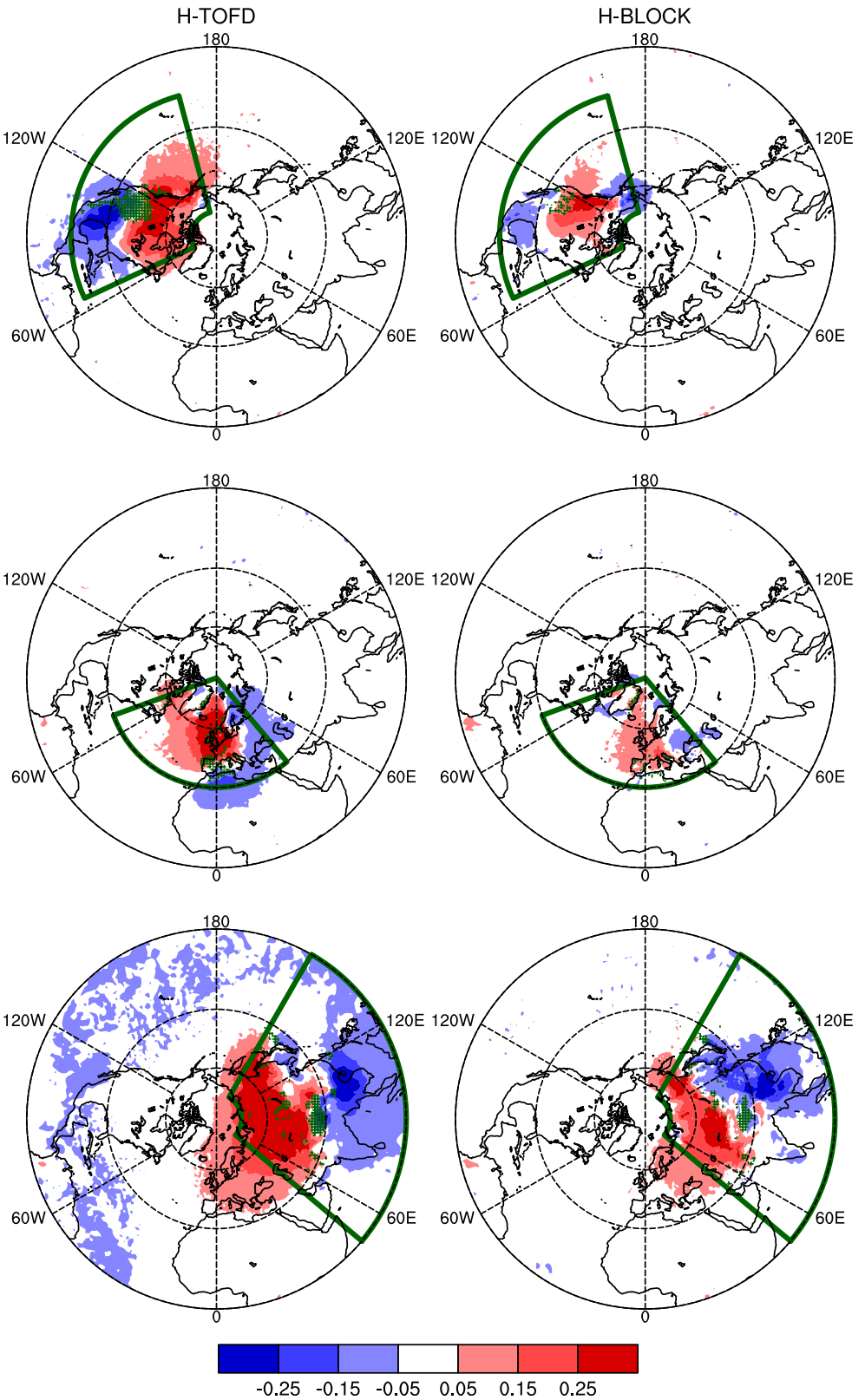

Figure 8. Mean change in surface pressure (hPa) in the experiments in which the TOFD, respectively, the BLOCK stress, are enhanced only in the regions demarked by the dark green lines, with respect to the CTL, at lead time 24 of the daily 00UTC forecasts performed for February 2014. The dark green hatches (from −1 to 0 m/s, by 0.25 m/s) indicate the deceleration of surface westerlies on the west side of the mountain ranges.

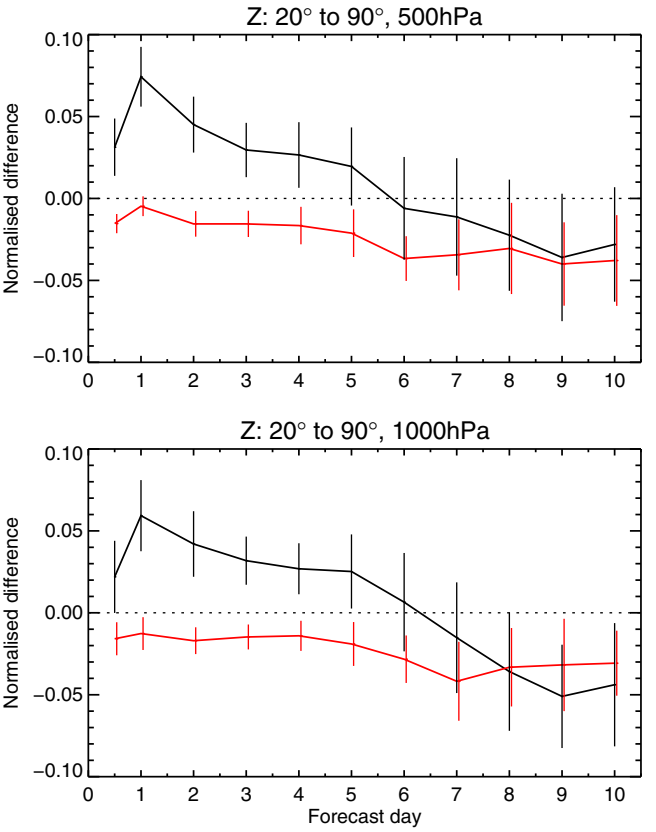

Figure 9. Relative difference of root mean square error (RMSE) of 500 and 1000 hPa geopotential height, between the H-TOFD (black), respectively, H-BLOCK (red), and the CTL forecasts, as a function of lead time. When error bars do not cross the zero line, the performance of the respective experiment is significantly worse/better (95% interval) than the CTL. For both the experiments and the CTL forecasts the RMSE was computed with respect to the analysis from which the forecasts started. A positive difference in RMSE indicates a deterioration of the model performance in the experiment with respect to the CTL.

4.2. Impacts on the NH Circulation in Medium-Range Forecasts

After 5 days, the changes to the TOFD scheme lead to an overall increase of the surface pressure at high latitudes and a decrease at low latitudes. This signal is less pronounced in the H-BLOCK experiment (Figure 7). The impacts on the zonal mean wind and temperature are also qualitatively similar, yet much stronger in the H-TOFD experiment (not shown). These results corroborate the findings of *Zadra et al.* [2003], who discussed in detail the impacts of introducing the low-level blocking parameterization of *Lott and Miller* [1997] in the GEM model used at the Canadian Meteorological Centre. This study demonstrated that the introduction of the blocking scheme leads to a weakening of the midlatitude westerlies in the NH during wintertime, the flow being affected up to approximately 150 hPa by day 5 of the forecasts (see their Figure 6). It also induces a change in zonal mean temperature at latitudes higher than 40°N characterized by a low-level warming and upper level cooling that also reaches 100 hPa by day 5 (see their Figure 9).

The effects obtained when increasing the TOFD stress are stronger in all circulation aspects examined so far. The impact on the forecast performance is hence bigger in the H-TOFD experiment (Figure 9). What is surprising however is that the change made to the TOFD stress considerably degrades the ability of the model to reproduce the NH circulation in the entire troposphere, while that made to the BLOCK stress leads to a slight improvement of the model performance. As illustrated by the increase, respectively, the reduction of the root mean square error of the geopotential height at 1000 and 500 hPa in Figure 9, these impacts are significant up to day 5 for the H-TOFD, and day 10 for the H-BLOCK experiment.

5. Impacts at Longer Time Range

In the previous section we showed that the partitioning of τ_{tot} between the TOFD and BLOCK schemes matters for the representation of the NH winter circulation in 10 day weather forecasts. In this section we investigate if this partition is also important at longer time ranges. We do that by analyzing the mean changes in circulation over the 30 winter (DJF) seasons simulated in the seasonal integrations described in section 3. Given that the runs start on 1 August, the examined lead time is between 4 and 7 months, which is similar to lead times of relevance for seasonal forecast integrations.

In both the H-TOFD-CL and H-BLOCK-CL experiments, the mean changes in surface pressure over these 30 DJF seasons (Figure 10, top) resemble those after 5 days of integration in the H-TOFD experiment (Figure 7) in that they show an increase in surface pressure at high latitudes and a decrease in the midlatitudes. However, this change in the meridional pressure gradient is particularly strong over the North Atlantic, where it resembles a negative phase of the North Atlantic Oscillation. Although these changes seem at first sight stronger in

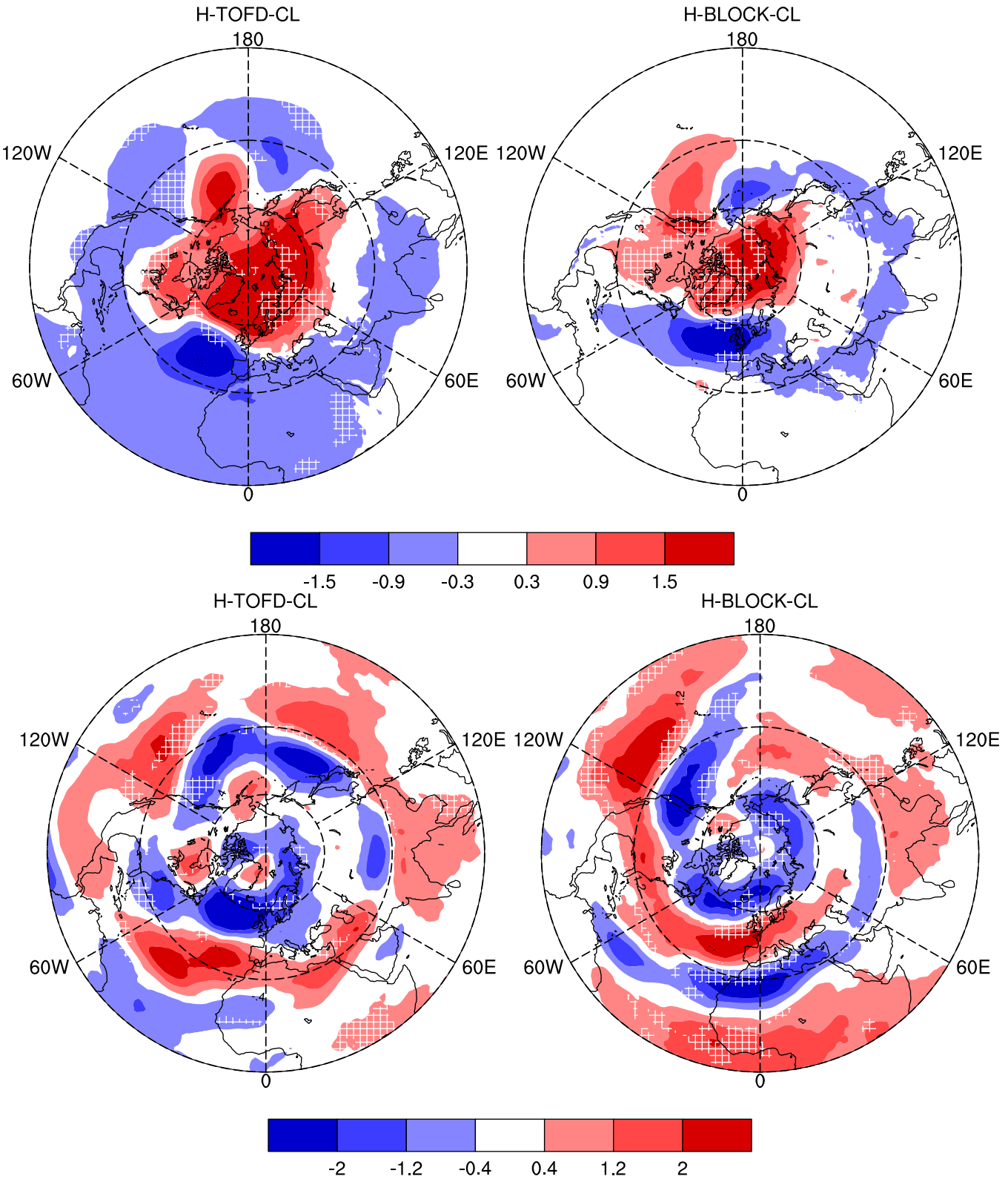

Figure 10. Mean change in surface pressure (hPa) (top row) and zonal wind at 200 hPa (m/s) (bottom row) in H-TOFD-CL and H-BLOCK-CL with respect to the CTL-CL experiment over the 30 DJF seasons (1984–2014). The horizontal white pattern (gridded areas) indicate 90 (95)% statistical significance according to a paired *t* test.

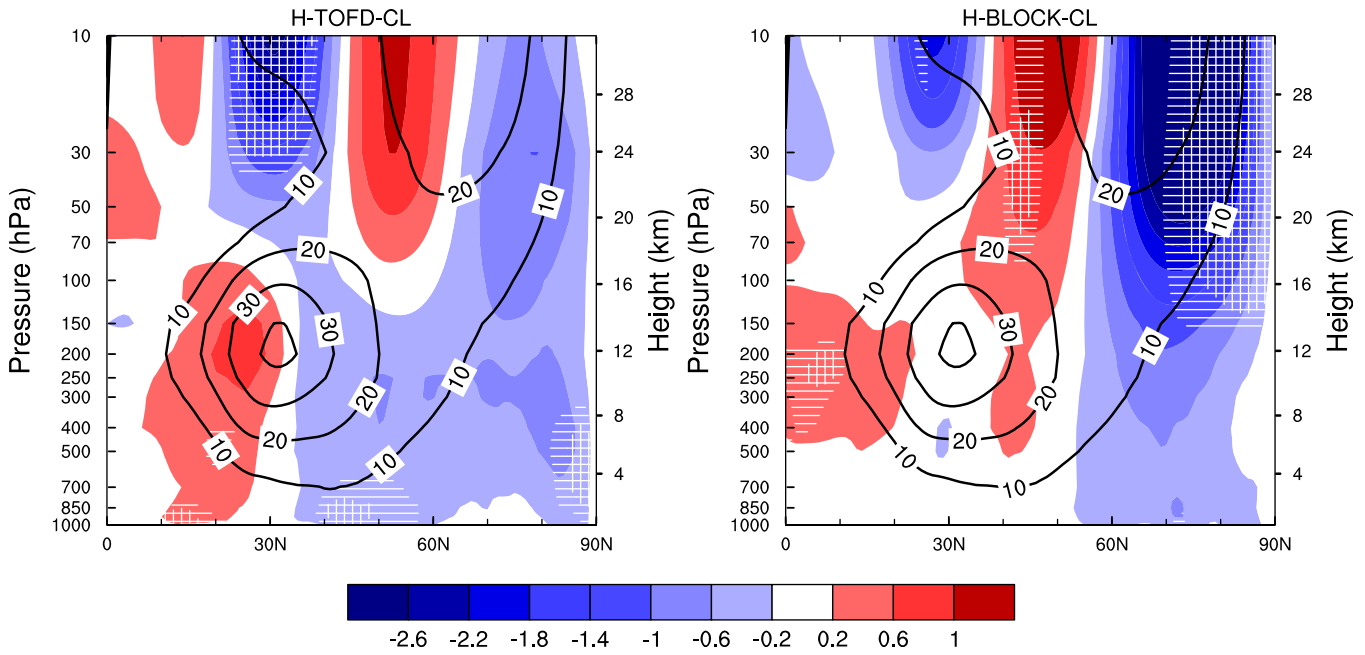

Figure 11. Mean change in zonal mean zonal wind (m/s, contours) in H-TOFD-CL (left) and H-BLOCK-CL (right) with respect to the CTL-CL experiment over the 30 DJF seasons (1984–2014). The horizontal white pattern (gridded areas) indicate 90 (95)% statistical significance according to a paired *t* test. The black lines show the zonal mean zonal wind in the CTL experiment.

the H-TOFD-CL experiment, the regions in which they are statistically significant (according to a 95% significance level computed with a regular paired *t* test) are less wide spread than in the H-BLOCK-CL experiment.

The effects of orographic low-level drag on the upper tropospheric zonal winds are illustrated in Figure 10 (bottom). The flow changes suggest that the increase in τ_{tot} affects the subtropical jets in both experiments, especially over the North Atlantic and North Pacific, where the southward displacement of the storm tracks is most pronounced. Interestingly, there are important differences between the responses over Europe, where climate models can show large biases in storm track location [*Zappa et al*., 2013].

Changes in the zonal mean zonal wind are also seen in the stratosphere in both experiments (Figure 11). Albeit weaker, the impacts on stratospheric winds are similar to those obtained by *Sigmond and Scinocca* [2010] when enhancing the orographic gravity wave momentum flux (see their Figure 3). Their study showed that increased orographic gravity wave momentum flux produces a basic state with weaker midlatitude winds in the wintertime lower stratosphere. Furthermore, it demonstrated that the deceleration of the lower stratospheric winds is related to changes in the resolved waves. Thus, an increased gravity wave drag strengthens the barrier to the equatorward propagation of planetary waves occurring in the midlatitude lower stratosphere. Consequently, the equatorward Eliassen-Palm (EP) flux is reduced and the planetary wave driving of the mid to high-latitude stratosphere is increased, leading to a deceleration of the polar stratospheric winds. By downward control arguments changes in the stratospheric circulation eventually affect the tropospheric circulation [*Haynes et al*., 1991].

Our experiments show a deceleration of the zonal winds on the poleward flank of the stratospheric polar vortex and a slight acceleration on its equatorward flank (Figure 11). These changes however appear to be statistically significant only in the H-BLOCK-CL experiment. In the H-TOFD-CL experiment, the only significant changes are found in the lower troposphere and midlatitude stratosphere.

In order to understand if these changes in stratospheric winds can also be explained by changes in the resolved wave driving, we performed an EP flux analysis similar to that of *Sigmond and Scinocca* [2010]. A Transformed Eulerian Mean (TEM) momentum balance was used to analyze the forcing of the zonally averaged flow by transient plus stationary eddies, following *Andrews et al*. [1987]; and the components of the EP flux, which is a direct measure of the total forcing of the zonal-mean state by the eddies [*Edmon et al*., 1980], were computed. The resulting EP flux arrows for the CTL-CL experiment are displayed in Figure 12 (left).

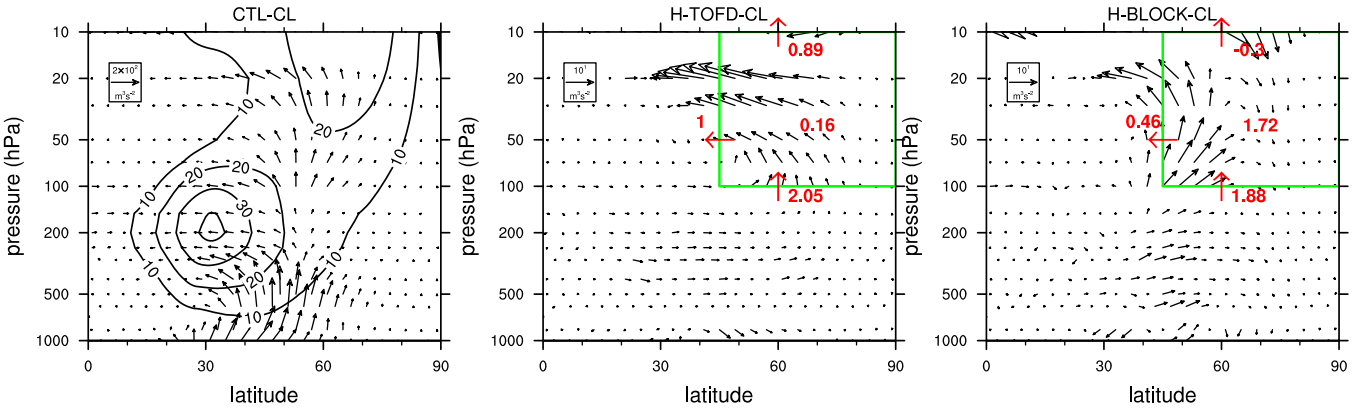

Figure 12. (left) EP-flux (arrows) and zonal mean zonal wind (contours, m/s) in the CTL-CL experiment for the 30 DJF seasons (1984–2014). (center/right) Change in EP-flux (arrows) in H-TOFD-CL, respectively, H-BLOCK-CL with respect to the CTL-CL experiment over the 30 DJF seasons. For clearer visualization the EP flux arrows have been scaled by the relative ranges of the two axes of the plot (3.14 radians by 10^5 Pa). The visibility of vectors in the stratosphere has been further enhanced by using a scaling factor proportional to the square-root of pressure and by applying a magnifying factor (of 3) above 100 hPa. A budget for resolved wave driving is presented for the stratospheric box between 100 and 10 hPa and between 45°N and 90°N. Red numbers across the box represent differences of EP fluxes integrated over the box boundaries between the H-TOFD-CL/H-BLOCK-CL and the CTL-CL experiment, while the red numbers in the box represent the differences in time and area-mean momentum deposition, or EP flux divergence, associated with the resolved waves (all wave numbers) within the box (10^4 kg ms^{-4}).

We then integrated the EP flux following *Kushner and Polvani* [2004, equation (7)] over a box bounded by 100 and 10 hPa and 45–90°N (green lines in Figure 12, middle, right). The red numbers on the sides of the box represent the difference in the integrated EP flux through the respective boundary, between each experiment and the CTL-CL. The values in Figure 12 suggest that for both experiments the amount of upward EP flux from the troposphere into the stratosphere across the 100 hPa boundary increases, and so does the equatorward EP flux across the 45°N boundary. In the H-BLOCK-CL experiment the upward EP flux through the 10 hPa surface decreases slightly, while in the H-TOFD-CL it increases by an amount comparable to the increase across the 45°N boundary. Overall, the H-BLOCK-CL experiment shows thus an increased momentum deposition, or EP flux convergence, in the polar stratosphere, while in the H-TOFD-CL experiment this resolved wave driving changes little compared to the CTL-CL experiment. This larger momentum deposition explains why the deceleration of winds at latitudes North of 60° N is stronger (and statistically more robust) in the H-BLOCK-CL experiment than in the H-TOFD-CL one (Figure 11). The differences in EP flux also explain the deceleration of the zonal winds above 30 hPa observed around 30°N in both experiments. The stronger deceleration observed in the H-TOFD-CL experiment appears to be associated with a stronger EP flux convergence at 20–30 hPa between 30°N and 40°N.

The analysis of the differences in various aspects of the NH winter circulation over the 30 DJF seasons suggests that the partitioning of the subgrid orographic low-level drag between the TOFD and BLOCK schemes is also important at longer time scales. While both schemes affect the circulation in the entire atmosphere, the details of these effects depend on which scheme represents the drag. The BLOCK scheme leads to effects somewhat similar, albeit weaker, than those of the GWD scheme discussed in *Sigmond et al*. [2008] and *Sigmond and Scinocca* [2010]. In contrast to those studies, the increased high-latitude stratospheric wave drag in H-BLOCK-CL is caused by more upward wave activity entering the region (Figure 12), rather than by less equatorward wave activity leaving the region [see *Sigmond and Scinocca*, 2010, Figure 6]; in other words, the changes are induced from below rather than from within the stratosphere. The turbulent orographic form drag on the other hand affects more strongly the lower troposphere and only partly the lower stratosphere. Finally, note that the main contribution to the EP flux in the stratosphere is due to wave numbers 1-5, while the main contribution to the tropospheric EP flux is by wave numbers greater than 5 (not shown). Therefore, the orographic form drag mainly affects the synoptic eddies while the low-level blocking affects the large-scale waves.

6. Conclusions

The representation of surface stress is important for accurately simulating the large-scale circulation in both weather forecasts and climate predictions. The first results of the ongoing WGNE Drag project revealed that state-of-the-art weather forecast models differ significantly in terms of the magnitude of the total subgrid

surface stress, especially over land and more particularly over orography. These differences concern both diurnal averages and details of the diurnal cycle. Furthermore, models also differ in the partitioning of this stress among the different parameterization schemes.

In the present study we tried to answer two questions raised by this intercomparison. We investigated the impact of changing τ_{tot} in a particular model by an amount comparable to the intermodel spread found in the WGNE Drag project. The discussion focuses on changes in the representation of the NH wintertime circulation in 10 day weather forecasts and seasonal integrations. Furthermore, we examined the impact of varying the partitioning of this increase in τ_{tot} between two schemes representing subgrid orographic drag, the turbulent orographic form drag and the low-level blocking schemes. These schemes have been chosen as the representation of orographic drag processes is still uncertain, and their impacts have been only poorly documented in the literature. The experiments designed to address these questions consisted in increasing the zonal mean τ_{tot} by 10–15% in the NH midlatitudes, via an increase in either the TOFD or the BLOCK contributions.

Such an increase in τ_{tot} was shown to significantly affect various aspects of the NH winter circulation both in 10 day forecasts and in longer integrations, irrespectively of which scheme is modified. Thus, changes in surface pressure are seen in all experiments and at all examined time scales, ranging from a few hours to a few months. A meridional surface pressure gradient across the large mountain chains is visible after a few hours of integration. These changes are induced through geostrophic balance as a response to the deceleration of the midlatitude surface westerlies caused by the enhancement of orographic stress. At longer time ranges, the surface pressure generally increases at high latitudes and decreases in the midlatitudes. The enhanced orographic stress also results in changes in the zonal wind, temperature, and geopotential at all time scales. The amplitude and robustness of the changes in surface pressure, winds and temperature depend however on the particular scheme which is modified.

Interestingly, in 10 day forecasts the increase in TOFD stress has a much stronger impact on the circulation than that in BLOCK stress, while the impact is of comparable magnitude for the seasonal integrations. More surprisingly, although both simulate an increase in stress over orography the changes to the TOFD and BLOCK schemes have opposite impacts in terms of medium-range forecast skill. The TOFD changes lead to a considerable degradation of the geopotential height skill in the troposphere (up to 200 hPa) up to day 5, while the BLOCK changes slightly improve the performance throughout the entire forecast range.

The seasonal integrations suggest that the two schemes have also different effects in terms of the model climate for the DJF season. The increase in BLOCK stress results in a significant deceleration of the zonal wind on the poleward flank of the stratospheric polar vortex by changing the resolved wave driving of the mid to high-latitude stratosphere. This was confirmed by an EP flux analysis similar to that performed by *Sigmond and Scinocca* [2010]. The changes to the TOFD scheme on the other hand mainly affect the lower troposphere and the midlatitude stratosphere.

In summary, these results suggest that the representation of the NH winter circulation is sensitive not only to changes in the total subgrid (orographic) stress, but also to the partitioning of this stress among different schemes. This is observed at both daily and seasonal time scales. The reasons for the different circulation response to the partitioning of the total surface stress remain to be understood. The different impacts of the two schemes discussed here could be related to inherent differences in their formulations, i.e., stability versus non stability dependence, the diurnal cycle and the horizontal scales on which they act.

Acknowledgments
We thank Adrian Lock and Andy Brown for access to the UM data submitted to the WGNE Drag project. The forecast data discussed in this study are available upon contacting the first author. F.P. acknowledges funding from the European Unions Horizon 2020 research and innovation program under the Marie Sklodowska-Curie grant 654492-UACSURF. T.G.S. is supported by an Advanced grant from the European Research Council.

References

Andrews, D. G., J. R. Holton, and C. B. Leovy (1987), *Middle Atmosphere Dynamics*, Acad. Press, San Diego, Calif.
Beljaars, A., A. Brown, and N. Wood (2004), A new parameterization of turbulent orographic form drag, *Q. J. R. Meteorol. Soc.*, *130*, 1327–1347.
Brown, A., and S. Webster (2004), Orographic flow-blocking scheme characteristics, *Q. J. R. Meteorol. Soc.*, *130*, 3015–3028.
Charney, J., and A. Eliassen (1949), A numerical method for predicting the perturbations of the middle latitude westerlies, *Tellus*, *1*(2), 38–54.
Chen, G., I. M. Held, and W. A. Robinson (2007), Sensitivity of the latitude of the surface westerlies to surface friction, *J. Atmos. Sci.*, *64*, 2899–2915.
Dee, D., et al. (2011), The era-interim reanalysis: Configuration and performance of the data assimilation system, *Q. J. R. Meteorol. Soc.*, *137*(656), 553–597.
Edmon, H., Jr., B. J. Hoskins, and M. E. McIntyre (1980), Eliassen-palm cross sections for the troposphere, *J. Atmos. Sci.*, *37*(12), 2600–2616.
Haynes, P. H., M. McIntyre, T. Shepherd, C. Marks, and K. P. Shine (1991), On the downward control of extratropical diabatic circulations by eddy-induced mean zonal forces, *J. Atmos. Sci.*, *48*, 651–678.

Held, I. M., M. Ting, and H. Wang (2002), Northern winter stationary waves: Theory and modeling, *J. Clim.*, *15*(16), 2125–2144.
Holton, J. (2004), *An Introduction to Dynamic Meteorology*, Elsevier Acad. Press., San Diego, Calif.
IFS documentation (2015), CY41r1, ECMWF. [Available at https://software.ecmwf.int/wiki/display/IFS/CY41R1+Official+IFS+Documentation#CY41R1OfficialIFSDocumentation-IV.Physicalprocesses.]
Kushner, P. J., and L. Polvani (2004), Stratosphere-troposphere coupling in a relatively simple AGCM: The role of eddies, *J. Clim.*, *17*(3), 629–639.
Lott, F. (1999), Alleviation of stationary biases in a GCM through a mountain drag parameterization scheme and a simple representation of mountain lift forces, *Mon. Weather Rev.*, *127*, 788–801.
Lott, F., and M. Miller (1997), A new subgrid orographic drag parameterization: Its formulation and testing, *Q. J. R. Meteorol. Soc.*, *123*, 101–127.
McFarlane, N. (1987), The effect of orographically excited gravity wave drag on the general circulation of the lower stratosphere and troposphere, *J. Atmos. Sci.*, *44*, 1775–1800.
McLandress, C., and N. McFarlane (1993), Interactions between orographic gravity wave drag and forced stationary planetary waves in the winter northern hemisphere middle atmosphere, *J. Atmos. Sci.*, *50*, 1966–1990.
Palmer, T. N., G. Shutts, and R. Swinbank (1986), Alleviation of a systematic westerly bias in general circulation and numerical weather prediction models through an orographic gravity wave drag parametrization, *Q. J. R. Meteorol. Soc.*, *112*, 1001–1039.
Pithan, F., W. Angevine, and T. Mauritsen (2015), Improving a global model from the boundary layer: Total turbulent energy and the neutral limit Prandtl number, *J. Adv. Model. Earth Syst.*, *7*, 791–805, doi:10.1002/2014MS000382.
Robinson, W. A. (1997), Dissipation dependence of the jet latitude, *J. Clim.*, *10*, 176–182.
Sandu, I., A. Beljaars, P. Bechtold, T. Mauritsen, and G. Balsamo (2013a), Why is it so difficult to represent stably stratified conditions in numerical weather prediction (NWP) models?, *J. Adv. Model. Earth Syst.*, *5*, 117–133, doi:10.1002/jame.20013.
Sandu, I., A. Beljaars, and G. Balsamo (2013b), Improving the representation of stable boundary layers, *ECMWF Newsl.*, *138*, 24–29.
Shaw, T., M. Sigmond, T. Shepherd, and J. Scinocca (2009), Sensitivity of simulated climate to conservation of momentum in gravity wave drag parameterization, *J. Clim.*, *22*, 2726–2742.
Sigmond, M., and J. F. Scinocca (2010), The influence of the basic state on the northern hemisphere circulation response to climate change, *J. Clim.*, *23*, 1434–1446.
Sigmond, M., J. F. Scinocca, and P. J. Kushner (2008), Impact of the stratosphere on tropospheric climate change, *Geophys. Res. Lett.*, *35*, L12706, doi:10.1029/2008GL033573.
Wallace, J. M., S. Tibaldi, and A. J. Simmons (1983), Reduction of systematic forecast errors in the ECMWF model through the introduction of an envelope orography, *Q. J. R. Meteorol. Soc.*, *109*, 683–717.
Webster, S., A. Brown, D. Cameron, and C. Jones (2003), Improvements to the representation of orography in the met office unified model, *Q. J. R. Meteorol. Soc.*, *129*, 1989–2010.
Wood, N., A. Brown, and F. Hewer (2001), Parametrizing the effects of orography on the boundary layer: An alternative to effective roughness lengths, *Q. J. R. Meteorol. Soc.*, *127*, 759–777.
Zadra, A. (2015), WGNE drag project: An inter-model comparison of surface stresses, technical report [Available at http://collaboration.cmc.ec.gc.ca/science/rpn/drag_project/documents/wgne_drag_project_report01.pdf]
Zadra, A., M. Roch, S. Laroche, and M. Charron (2003), The subgrid-scale orographic blocking parametrization of the gem model, *Atmos. Ocean*, *41*, 155–170.
Zappa, G., L. Shaffrey, and K. Hodges (2013), The ability of CMIP5 models to simulate north Atlantic extratropical cyclones, *J. Clim.*, *26*, 5379–5396.